JAERI-M
6124

# DIFFUSION IN A TOKAMAK WITH HELICAL MAGNETIC CELLS

May 1975

Masahiro WAKATANI

日本原子力研究所
Japan Atomic Energy Research Institute

この報告書は，日本原子力研究所が JAERI-M レポートとして，不定期に刊行している研究報告書です．入手，複製などのお問合わせは，日本原子力研究所技術情報部（茨城県那珂郡東海村）あて，お申しこしください．

JAERI-M reports, issued irregularly, describe the results of research works carried out in JAERI. Inquiries about the availability of reports and their reproduction should be addressed to Division of Technical Information, Japan Atomic Energy Research Institute, Tokai-mura, Naka-gun, Ibaraki-ken, Japan.

JAERI-M 6124

# Diffusion in a Tokamak with Helical Magnetic Cells

Masahiro WAKATANI

Thermonuclear Fusion Laboratory, Tokai, JAERI

(Received April 18, 1975)

In a tokamak with helical magnetic cells produced by a resonant helical magnetic field, diffusion in the collisional regime is studied. The diffusion coefficient is greatly enhanced near the resonant surface even for a weak helical magnetic field. A theoretical model for disruptive instabilities based on the enhanced transport due to helical magnetic cells is discussed. This may explain experiments of the tokamak with resonant helical fields qualitatively.

JAERI－M 6124

# ヘリクル・マグネティク・セルのあるトカマクにおける拡散

日本原子力研究所東海研究所核融合研究室

若谷誠宏

（1975年4月18日受理）

共鳴ヘリカル磁場によるヘリカル・マグネティク・セルのあるトカマクにおいて，MHD 領域の拡散を調べる。拡散係数は，弱いヘリカル磁場であっても共鳴点の近傍で大きくなる。ヘリカル・マグネティク・セルによる輸送現象に基くディスラプティブ不安定の理論的モデルについて論じる。これは共鳴ヘリカル磁場のあるトカマクの実験に定性的な説明を与える。

## §1. Introduction

In a cylindrical plasma column with sheared magnetic field, $\underset{\sim}{B} = (0, B_\theta(r), B_z = \text{const.})$, a perturbed helical magnetic field $\underset{\sim}{b}$ produces helical magnetic cells in the neighborhood of $r_s$, if the pitch of the helical field $2\pi/f$ coincides with the pitch of the helical lines of force of the unperturbed field $2\pi/\mu = 2\,(rB_z/B_\theta)$ at the resonant surface $r_s$ [1]. This helical field is called as a resonant helical field. In a tokamak plasma, resistive tearing instabilities may produce helical magnetic cells for $q(r_s) = m/n$, where q is a safety factor and m, n are integers[2].

When the plasma column has helical magnetic cells inside, it may be considered that the transport rate of plasma near $r_s$ is greatly enhanced. In the banana regime, Krommes and Rutherford[3] calculated neoclassical particle diffusion for a tokamak with helically perturbed magnetic fields. They showed that the diffusion coefficient due to perturbed helical fields becomes larger near the resonant surface. In the collisional regime, Ohkawa[4] obtained the enhancement factor in diffusion coefficient which becomes large when the helix $m\theta - kz = \text{const.}$ is parallel to the magnetic field, i.e. $B_\theta + k/m\, B_z \longrightarrow 0$. In §2, we will study convective flow for a tokamak with resonant helical magnetic fields and find the diffusion coefficient in the collisional regime.

Recently Ohkawa[5] proposed a theoretical model for disruptive instabilities in a tokamak, by considering the rapid transport near $r_s$ and that the plasma will move the poloidal magnetic flux but leave the toroidal magnetic flux alone. In §3, we will investigate this problem by use of numerical calculations.

The experiments of Pulsator I, the tokamak with helical windings of $\ell = 2$, showed that the resonant helical field corresponding to $J_h^*$ induces always current disruption and there may be some correlation between helical magnetic cells and the disruptive instabilities[6], where $J_h^*$ denotes a critical helical current. In §4, we will try to explain these experiments by the results obtained in §3.

## §2. Convective Flow in a Helically Perturbed Tokamak

The convective flux in a tokamak with a perturbed helical field $\underset{\sim}{b}$ is calculated. Here the unperturbed magnetic field is given by $\underset{\sim}{B}_o = (0, B_\theta^o(r), B_\zeta)$, $B_\zeta = B_\zeta^o(1 - r/R \cos\theta)$. We start from the two fluids equations and neglect the inertia,

$$-\nabla P_i - en\nabla\phi + en\underset{\sim}{v}_i \times \underset{\sim}{B} - m_e \nu_{ei} n(\underset{\sim}{v}_i - \underset{\sim}{v}_e) - nm_i \nu_{io} \underset{\sim}{v}_i = 0 \qquad (1)$$

$$-\nabla P_e + en\nabla\phi - en\underset{\sim}{v}_e \times \underset{\sim}{B} + m_e \nu_{ei} n(\underset{\sim}{v}_i - \underset{\sim}{v}_e) = 0 \qquad (2)$$

$$\text{div } n\underset{\sim}{v}_i = Q \qquad (3)$$

$$\text{div } n\underset{\sim}{v}_e = Q \,, \qquad (4)$$

where n is plasma density, $\underset{\sim}{B} = \underset{\sim}{B}_o + \underset{\sim}{b}$, $P_i$ is ion pressure, $P_e$ is electron pressure and Q is a source term for electrons and ions. In eq. (1) $\nu_{io}$ means ion neutral collision frequency and we have assumed that neutral particles have no macroscopic motion. In a tokamak, $10^8$ ~ $10^9$ $cm^{-3}$ neutral particles exist in steady state discharge[7] and the above model may be resonable in the collisional regime of present tokamak. It will be shown later that the momentum exchange with neutral particles is necessary only in the neighborhood of resonant surface to prevent divergence of the diffusion coefficient. In a tokamak, inductive electric field driving toroidal current is nearly parallel to the magnetic lines of force and constant in the steady state. Then it dose not affect the convective flow, we have omitted the inductive electric field in eqs. (1) and (2). In eqs. (1) and (2), $\phi$ denotes electrostatic potential.

We solve eqs. (1) ∿ (4) by following the analysis given by Wobig[8]. We assume $T_e = T_i = T$ = const. to study diffusion process. As $\nu_{ei} \ll \Omega_e$ and $\nu_{io} \ll \Omega_i$, the velocities of ion and electron are found from eqs. (1) and (2),

$$\underset{\sim}{v}_{i1} = \frac{\nabla\Psi_i \times \underset{\sim}{B}}{B^2} + (\alpha + \beta)\frac{\nabla_1\Psi_i}{B^2} + \beta\frac{\nabla_1\Psi_e}{B^2} \qquad (5)$$

$$\underset{\sim}{v}_{e1} = -\frac{\nabla\Psi_e \times \underset{\sim}{B}}{B^2} + \beta\frac{\nabla_1\Psi_e}{B^2} + \beta\frac{\nabla_1\Psi_i}{B^2} \qquad (6)$$

$$\underset{\sim}{v}_{e11} = (\nabla_{11}\Psi_i + \nabla_{11}\Psi_e)/\alpha \qquad (7)$$

$$\underset{\sim}{v}_{e11} = (\nabla_{11}\Psi_i + \nabla_{11}\Psi_e)/\alpha + \nabla_{11}\Psi_e/\beta \ , \tag{8}$$

where $\Psi_i = -T/e \ \ell n \ n/\bar{n} - \phi$, $\Psi_e = -T/e \ \ell n \ n/\bar{n} + \phi$ and $\alpha = m_i\nu_{io}/e$, $\beta = m_e\nu_{ei}/e$. Here $\bar{n}$ is the reference density and $v_\perp$ and $v_{11}$ denote perpendicular and parallel to $\underset{\sim}{B}$ respectively. It should be noted that the ion neutral collision frequency makes it possible to obtain $v_{i11}$ and $v_{e11}$. From the equations of continuity (3), (4), we find

$$\mathrm{div}\left(\frac{\beta T}{B^2 e}\nabla_\perp n + \frac{T}{\alpha e}\nabla_{11} n + n\frac{\nabla\phi\times\underset{\sim}{B}}{B^2}\right) = -Q \tag{9}$$

$$\mathrm{div}\left(\frac{\alpha\beta}{B^2}\nabla_\perp\phi + \frac{n}{\beta}\nabla_{11}\phi + \frac{\alpha T}{eB^2}\nabla_\perp n - \frac{T}{e\beta}\nabla_{11} n + \frac{2T}{e}\frac{\nabla n\times\underset{\sim}{B}}{B^2}\right) = 0 \ , \tag{10}$$

when we go back to $\phi$ and n, where $\alpha \ll \beta$ (or $\nu_{io} \ll \nu_{ei}$) has been used. Here we consider that eq. (9) determines $\bar{n}$ if $\phi$ is given and eq. (10) determines $\phi$ if n is known.

We choose toroidal coordinates $(r, \theta, \zeta)$, where $r = \text{const.}$ denotes an unperturbed magnetic surface and $\varepsilon = r/R \ll 1$. As it may be considered that deviation from $\nabla_{11} n = 0$ is small and $O(\alpha/\beta)$ or $O(\nu_{io}/\Omega_i)$, the density profile may be considered as

$$n = n_0(r) + O(\nu_{io}/\Omega_i). \tag{11}$$

This means that the magnetic configuration is almost axisymmetric except that narrow resonant region. Then we may neglect the third and forth terms in the eq. (10) for $\alpha \ll \beta$. From eqs. (10) and (11),

$$\mathrm{div}\left(\frac{\alpha n_0}{B^2}\nabla_\perp{}^0\phi + \frac{n_0}{\beta}\nabla_{11}{}^0\phi + \frac{2T}{e}\frac{\nabla n_0\times\underset{\sim}{B}}{B^2}\right) = 0 \tag{12}$$

is found, where $\nabla_\perp{}^0$ and $\nabla_{11}{}^0$ are perpendicular and parallel derivative to $\underset{\sim}{B}_0$ respectively. Eq. (12) is the differential equation determing the electrostatic potential $\phi$. The first term of eq. (12) may be negligible in the region where no resonant surface exists. If the resonant surface exists, we must include the first term. The size of this resonant region is determined by the shear of the unperturbed magnetic field. Some rough estimates give

$$\mathrm{div}\ \frac{\alpha n_0}{B^2}\nabla_\perp{}^0\phi \sim \frac{\alpha n_0}{B_0^2}\frac{\phi}{x^2} \tag{13}$$

$$\mathrm{div}\,\frac{n_o}{\beta}\nabla_{11}{}^{o}\phi \sim \frac{n_o}{\beta}(\nabla_{11}{}^{o})^2\phi \sim \frac{n_o}{\beta}\left(\frac{q'}{q^2}\right)^2\frac{r_s^2}{R^2\lambda_\perp^2}\phi x^2 \quad , \tag{14}$$

where $x = |r - r_s|$, $q = rB_\zeta^o/RB_\theta^o$ and $\lambda_\perp$ is a measure of the inhomogeneity of $\phi$ on the magnetic surface. From (13) and (14) the size of the resonant region $\delta$ is found by

$$\delta^2 \sim \left(\frac{\alpha\beta}{B^2}\right)^{1/2}\lambda_\perp\frac{q^2}{|q'|}\frac{r_s}{R} = \lambda_\perp\frac{q^2}{|q'|}\frac{r_s}{R}\left(\frac{\nu_{io}}{\Omega_i}\frac{\nu_{ei}}{\Omega_e}\right)^{1/2} \tag{15}$$

Outside the resonant region eq. (12) gives

$$\mathrm{div}\,\frac{\mu_o}{\beta}\nabla_{11}{}^{o}\phi + \frac{2T}{e}\nabla n_o\times\mathbf{B}\cdot\nabla\left(\frac{1}{B^2}\right) - \frac{2T}{e}\frac{1}{B^2}\nabla n_o\cdot\mathbf{J} = 0 \ . \tag{16}$$

We consider the unperturbed magnetic configuration is nearly equal to MHD equilibrium $\mathbf{J}\times\mathbf{B}_o = T\nabla n_o$ and the third term of eq. (16) may be negligible. Noting $\nabla_{11}{}^{o} = (B_\theta^o/rB_\zeta^o\frac{\partial}{\partial\theta} + \frac{\partial}{\mu\zeta})\,\hat{e}_{11}$ for $\varepsilon \ll 1$ and $n_o/\beta$ is independent of r, we find

$$\frac{n_o}{\beta}\left(\frac{B_\theta^o}{rB_\zeta^o}\frac{\partial}{\partial\theta} + \frac{\partial}{\partial\zeta}\right)^2\phi + \frac{2T}{er}B_o\frac{dn_o}{dr}\frac{\partial}{\partial\theta}\left(\frac{1}{B^2}\right) = 0 \ . \tag{17}$$

Here we have neglected $0(\varepsilon^2)$ and $0\ (b^2)$. Eq. (17) can be solved by Fourier expansion. When the resonant helical fields have a pitch $f = n/mR$, $1/B^2$ and $\phi$ are periodic in $\theta$ and $\phi$ and

$$\frac{1}{B^2} = \Sigma\frac{g_{mn}}{4\pi^2R}e^{im\theta - in/R\zeta}$$

$$\phi = \Sigma\frac{\phi_{mn}}{4\pi^2R}e^{im\theta - in/R\zeta}$$

are given. By these expansions and eq. (17),

$$\phi_{mn} = im\frac{2TB_o}{er}\frac{\beta}{n_o}\frac{dn_o}{dr}\frac{R^2q^2}{(m-nq)^2}g_{mn} \tag{18}$$

is obtained.

Next in the resonant region, we solve the differential equation

$$-\frac{\alpha n_o}{B_o^2}\frac{d^2\phi_{mn}}{dx^2} + \frac{n_o}{\beta}\frac{q'^2}{q^4}\frac{m^2}{R^2}\phi_{mn}x^2 = \frac{2TB_o}{er}\frac{dn_o}{dr}im\,g_{mn}, \tag{19}$$

With the approximation $d^2\phi_{mn}/dx^2 \sim -\phi_{mn}/\delta^2$, the solution of eq. (19) is

given by

$$\phi_{mn} \simeq \frac{im \dfrac{2TB_o}{er} \dfrac{\beta}{n_o} \dfrac{dn_o}{dr} R^2q^2}{\dfrac{q'^2}{q^2} r^2x^2 + \dfrac{\alpha\beta}{B_o^2} \dfrac{R^2q^2}{\delta^2}} g_{mn} \quad . \tag{20}$$

From (18) and (20), we obtain the approximate solution for $\phi_{mn}$ which is good on the resonant surface and at a large distance ($x \ll \delta$) from the resonant surface,

$$\phi_{mn} \simeq \frac{im \dfrac{2TB_o}{er} \dfrac{\beta}{n_o} \dfrac{dn_o}{dr} R^2q^2}{(m-nq)^2 + \eta} g_{mn} \quad , \tag{21}$$

where $\lambda_1 = r_s/m$ and

$$\eta = mR|q'| \left(\frac{\nu_{io}}{\Omega_i} \frac{\nu_{ei}}{\Omega_e}\right)^{1/2}$$

have been used.

The convective flow across a magnetic surface is given by the last term of L.H.S. of eq. (9). We will calculate the convective flow in the tokamak with resonant helical fields $\ell = s$ (integer) in the following procedure. When the effect of resonant helical fields is considered, the toroidal effects are neglected. For axisymmetric mode (n=0), we retain the toroidal effects in the lowest order. Using (21), we can find the convective flux

$$\Gamma_c = \frac{n_o}{4\pi^2 rR} \int \frac{\nabla\phi \times \tilde{B}}{B^2} dS = \frac{n_o B_o}{4\pi^2 rR} \int \frac{\partial\phi}{\partial\theta} \frac{1}{B^2} d\theta d\zeta$$

$$= -\sum_{\substack{m=1 \\ n=0}}^{\infty} \frac{2TB_o^2}{er^2} \beta n_o \frac{R^2q^2m^2|g_{mn}|^2}{(m-nq)^2 + \eta} \tag{22}$$

For the axisymmetric mode, neglecting the helical field

$$\frac{1}{B_o^2} \simeq \frac{1}{B_o^2}(1 + \frac{2r}{R}\cos\theta) \quad ,$$

we find

$$g_{10} = \frac{1}{B_o^2}\frac{r}{R} \quad . \tag{23}$$

For the $\ell = s$ resonant helical fields

$$b_r = \delta_r \sin s(\theta - f\zeta)$$
$$b_\theta = \delta_\theta \cos s(\theta - f\zeta)$$
$$b_\zeta = \delta_\zeta \cos s(\theta - f\zeta) \quad ,$$

neglecting the toroidal effects and retaing the fundamental mode

$$\frac{1}{B^2} \simeq \frac{1}{B_o^2}\left(1 - \frac{2b_\zeta}{B_o} - \frac{2B_\theta^o b_\theta}{B_o^2}\right) \quad ,$$

we find

$$g_{s1} \simeq -\frac{1}{B_o^2}\left(\frac{\delta_\zeta}{B_o} + \frac{B_\theta^o \delta_\theta}{B_o^2}\right) \quad , \tag{24}$$

where we have noted $f = 1/sR$.

Here it should be noted that $g_{10}$ gives

$$\Gamma_c = -2\nu_{ei}\rho_e^2 q^2 n_o' \tag{25}$$

by use of $\beta/B_o = \nu_{ei}/\Omega_e$. This shows the well-known Pfirsch Schlüter factor[9]. From (23) and (24) we obtain the convective flux in the presence of the $\ell = s$ resonant helical fields

$$\Gamma_c = -n_o' \frac{2TB_o^2}{er^2} q^2 R^2 \beta\left(|g_{10}|^2 + \frac{s^2|g_{s1}|^2}{(s-q)^2 + \eta}\right) \tag{26}$$

In the resonant region, the second term becomes dominant as $\eta$ is a sufficiently small quantity. From (26) the diffusion coefficient in a tokamak with $\ell = s$ resonant helical fields is given by

$$D_1 = 2\nu_{ei}\rho_e^2 q^2 B_o^4 \frac{R^2}{r^2}\left(|g_{10}|^2 + \frac{s^2|g_{s1}|^2}{(s-q)^2 + \eta}\right) \quad . \tag{27}$$

It should be noted that $\nu_{io}$ is included in only $\eta$. For $\nu_{io} \ll \Omega_i$, $\nu_{ei} \ll \Omega_e$, $\eta$ becomes very small and the second term becomes larger in the resonant region $q \sim s$, even though $|g_{10}| \gg |g_{s1}|$.

## §3. Current Profile of Tokamak with Helical Magnetic Cells

In this section, we assume that configuration is axisymmetric except the resonant region where the asymmetry due to perturbed helical magnetic fields causes the enhanced diffusion shown in §2. Then the Ohm's low for a tokamak is approximately

$$j_z = \sigma \left(E_z + \frac{\langle V_r \rangle B_\theta}{C}\right) , \tag{1}$$

where $\sigma$ is Spitzer conductivity and we have assumed $T_e = \text{const}$[10]. The diffusion velocity $\langle V_r \rangle$ is obtained from eq. (26) in §2,

$$\langle V_r \rangle = -\frac{2TB_\theta^2}{er^2}\frac{\beta}{n_o} q^2 R^2 \frac{dn_o}{dr}\left(|g_{10}|^2 + \frac{s^2|g_{s1}|^2}{(s-q)^2+\eta}\right) . \tag{2}$$

From Maxwell equations and eq. (1), we find

$$\frac{\partial B_\theta}{\partial t} = -\frac{\partial}{\partial r}\left(\langle V_r \rangle B_\theta\right) + \frac{\partial}{\partial r}\left[\frac{c^2}{4\pi\sigma}\frac{1}{r}\frac{\partial}{\partial r}(rB_\theta)\right] . \tag{3}$$

Here we put $\partial B_z/\partial r = 0$, which is valid in cylindrical approximation. We consider toroidal effects and the resonant helical fields only in the transport rate. In a tokamak the relation $B_\theta << B_z$ and incompressibility confirms $\text{div}_\perp \underset{\sim}{V} \simeq 0$. This is consistent with $\partial B_z/\partial t = 0$ which means that the plasma moves the poloidal magnetic flux but leave the toroidal magnetic flux.

We will solve eq. (3) as an initial value problem. Since $\langle V_r \rangle$ involve $B_\theta$ through q, eq. (3) is a non-linear differential equation. We use the Crank-Nicholson difference scheme to solve eq. (3) numerically. We have chosen the Pulsator I[6], R = 70 cm, a = 12 cm, $B_o$ = 30,000G, with the $\ell = 2$ resonant helical field, as a model tokamak. We assume $T_e$ = 500 eV uniformly to assure the assumption to obtain $\langle V_r \rangle$. The density is fixed at $n(o) = 5 \times 10^{13}$ cm$^{-3}$ and $n'/n = -18r/(9r^2 + a^2)$. For the parabolic current profile at t = 0, Fig. 1 is obtained, where q(a) = 3.5 is fixed as the boundary condition. The current profile is found by numerical derivative

$$J_z^i = \frac{1}{r_i}\frac{(rB_\theta)^{i+1} - (rB_\theta)^{i-1}}{2\Delta r} . \tag{3}$$

Fig. 1 shows the perturbation in the current profile which expands as time

elapses. The perturbed region of current profile has the safety factor $q(r) \simeq 2$. It may be considered that this shows expansion of helical magnetic cells. Locally rapid transport produces these perturbation and

$$\frac{\partial B_\theta}{\partial t} \sim \frac{\partial \langle V_r \rangle}{\partial r} B_\theta \qquad (4)$$

is dominant term of eq. (2) in the resonant region. Here it should be noted that $|g_{21}|$ is given by constant in space and time,

$$|g_{21}| = 0.0006/B_o^2 \quad , \qquad (5)$$

as $|g_{21}|$ contributes in the resonant region dominantly. We also choose $\eta = 10^{-5}$, i.e. $(\nu_{io}/\Omega_i \cdot \nu_{ei}/\Omega_e)^{1/2} \sim 10^{-6}$. This corresponds to helical magnetic filed b ~ 200G which may be 5 ~ 20 times larger than that of experiments in Pulsator I. This discrepancy is partly due to the scheme of numerical calculation. We divided a = 12 cm into 100 meshes, i.e. $\Delta r = 0.12$ cm which is of order of ion gyroradius. The variation of safety factor in one mesh near the resonant surface, $\Delta q$, is ~0.01. In the expression of $\langle V_r \rangle$, the second term gives $|g_{21}|^2/(\Delta q)^2 \gtrsim 10^4 |g_{21}|^2$ and the first term gives $|g_{21}|^2 \lesssim 10^{-2}$ near the resonant surface. The second term showing enhanced diffusion becomes larger for $|g_{21}| \gtrsim 10^{-3}$. In reality weaker resonant helical field than that used here, which produces helical magnetic cells smaller than the ion gyroradius, changes the diffusion coefficient drastically in the scale of electron gyroradius. Therefore we infer that the phenomena shown in Fig. 1 may appear for a weaker resonant helical field. We also interpret that the large helical field that used here includes anomalous diffusion coefficient due to electrostatic turbulence in the resonant region (which do not disturb $B_z$ field). The $|g_{21}|^2$ in our calculation corresponds to $\beta|\tilde{g}_{21}|^2$, where $\tilde{g}_{21}$ is due to external helical fields and $\beta \sim 100$ is the anomaly factor compared to the neoclassical diffusion in the axissymmetric torus. We consider that the above two considerations may assure to apply this model to tokamak experiments.

In addition the phenomena shown in Fig. 1 take place for other current profile concentrated in the magnetic axis. Fig. 2 shows the calculation of skin-like current profile with the same magnitude of resonant helical field, where

$$J_z \propto \exp(-4\,(\frac{r}{a} - 0.8)^2) \ .$$

Here q(a) = 1.5 is fixed and q(o) = 13.04 at t = 0. Fig. 2 shows locally rapid transport due to helical magnetic cells gives small perturbation in the current profile and may deteriorate confinement in a tokamak less than Fig. 1. This confirms Ohkawa's model which shows that a skin current profile is stable to disruptive instabilities.

## §4. Discussion about Disruptive Instabilities

In this section we will discuss the relation between numerical calculations shown in §3 and the disruptive instabilities. Current disruption is not induced by the perturbation of current profile shown in Fig. 1 only. The variation of internal inductance of the longitudinal current $J_z$[11], $\Delta\ell_i \sim 0.05$ per 1 msec, is small to make a large toroidal drift and the change of one turn voltage, $V = 2\pi R\, \partial\Psi_p/\partial t \sim -0.2$V/msec, is small to produce voltage spike, where $\Psi_p$ denotes poloidal flux. In a tokamak current channel shrinking due to thermal instability, impurities or neutral particles is usually occurs in steady state discharge[12]. Combining the current channel shrinking with the expansion of helical magnetic cells shown in Fig. 1, we may cinsider two explanations of disruptive instabilities.

i) Helical magnetic cells or resonant surface (q=2) moves outward and expand as the current channel shrinks and interact with limitter.

ii) With current channel shrinking, $q(o)$ becomes less than 1 and $m = 1$ internal link instability shifts the toroidal plasma column[13]. Then the expanded helical magnetic cells of $q = 2$ interact with the limitter.

It may be reasonable to consider that the disruptive instabilities appear by the mixture of the above two mechanisms. We consider that it will be essential to prevent excess shrinking of current channel to obtain stable discharge in low q(a).

Lastly we will interpret the interesting experiments of Pulsator I by the above discussed mechanisms. In the experiments of Pulsator I, resonant helical fields corresponding to $J_h^*$ induce always current disruption. When one applies a resonant helical field whose value lies between 60 ~ 90 (%) of $J_h^*$, the spontaneous disruptive instability can be avoided for a constant plasma current. We will assume that for $J_h^* = 0$, $m = 2$ tearing instability, which is observed experimentally, produces helical magnetic cells and q(o) becomes less than 1 by the current channel shrinking. For large $J_h \sim J_h^*$, the helical magnetic cells made by $J_h^*$ expand rapidly and interact the limitter. This interaction will induce current disruption. For fairly weak $J_h$, the helical magnetic cells expand $q \sim 2$ region as shown in Fig. 1. We infer this helical magnetic cells may weaken the current channel shrinking. However, when $q(o) \sim 1$ is reached, disruptive instability will be induced. Then the

plasma current duration is prolonged by this slower shrinking of the current channel. Conclusively, our model based on the rapid transport due to helical magnetic cells and the current channel shrinking may explain macroscopic behavior of experiments of Pulsator I qualitatively.

Acknowledgements

The auther would like to thank Dr. M. Tanaka and Prof. S. Hamada in Nihon University for variable discussions.

## References


1) A.I. Morozov and L.S. Solovev: Reviews of Plasma Physics, vol. 2, p.1. (Consultant Bureau, New York, 1965).
2) B.B. Kadomtsev and O.P. Pogutse: Reviews of Plasma Physics. vol.5, p.249 (Consultant Bureau, New York, 1970).
3) J.A. Krommes and P.H. Rutherford: Nuclear Fusion 14, 695 (1974).
4) T. Ohkawa: Physics Letters, 38A, No. 1, 21 (1972).
5) T. Ohkawa: GA Report A 13044 (1974).
6) F. Karger et. al. : IAEA Tokyo Conference (1974) CN-33/A8-2.
7) K. Bol et. al.: Phys. Rev. Letters 32, 661 (1974).
8) H. Wobig: Plasma Physics 15, 403 (1973).
9) D. Pfirsch and A. Schlüter: Max. Plank Institute Report MPI/PA/7/62 (1962).
10) A.A. Ware: Nucl. Fusion 13, 793 (1972).
11) V.D. Shafranov: Soviet-Physics.JETP 6, 545 (1958).
12) D.F. Düchs, H.P. Furth and P.H. Rutherford in Plasma Physics and Controlled Nuclear Fusion Research (IAEA, Vienna, 1971), vol. I, p.369.
13) M.N. Rosenbluth, R.Y. Dagazian and P.H. Rutherford: Phys. Fluids 16, 1894 (1973).

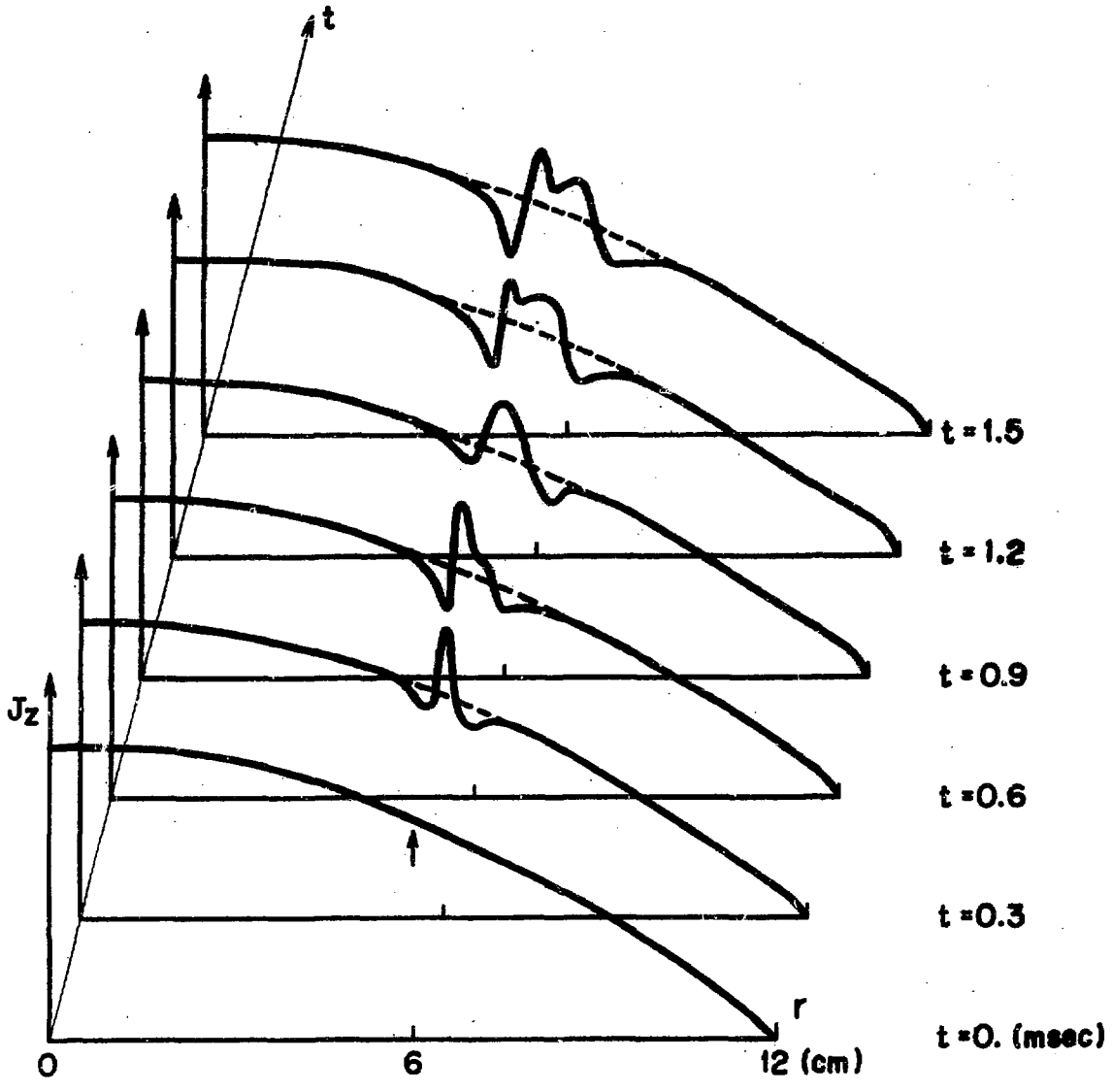


Fig. 1 Variation of toroidal current profile. The initial current profile is parabolic. The arrow at t = 0 indicates the position of q = 2 surface. The dotted lines show the case of $g_{21} = 0$.

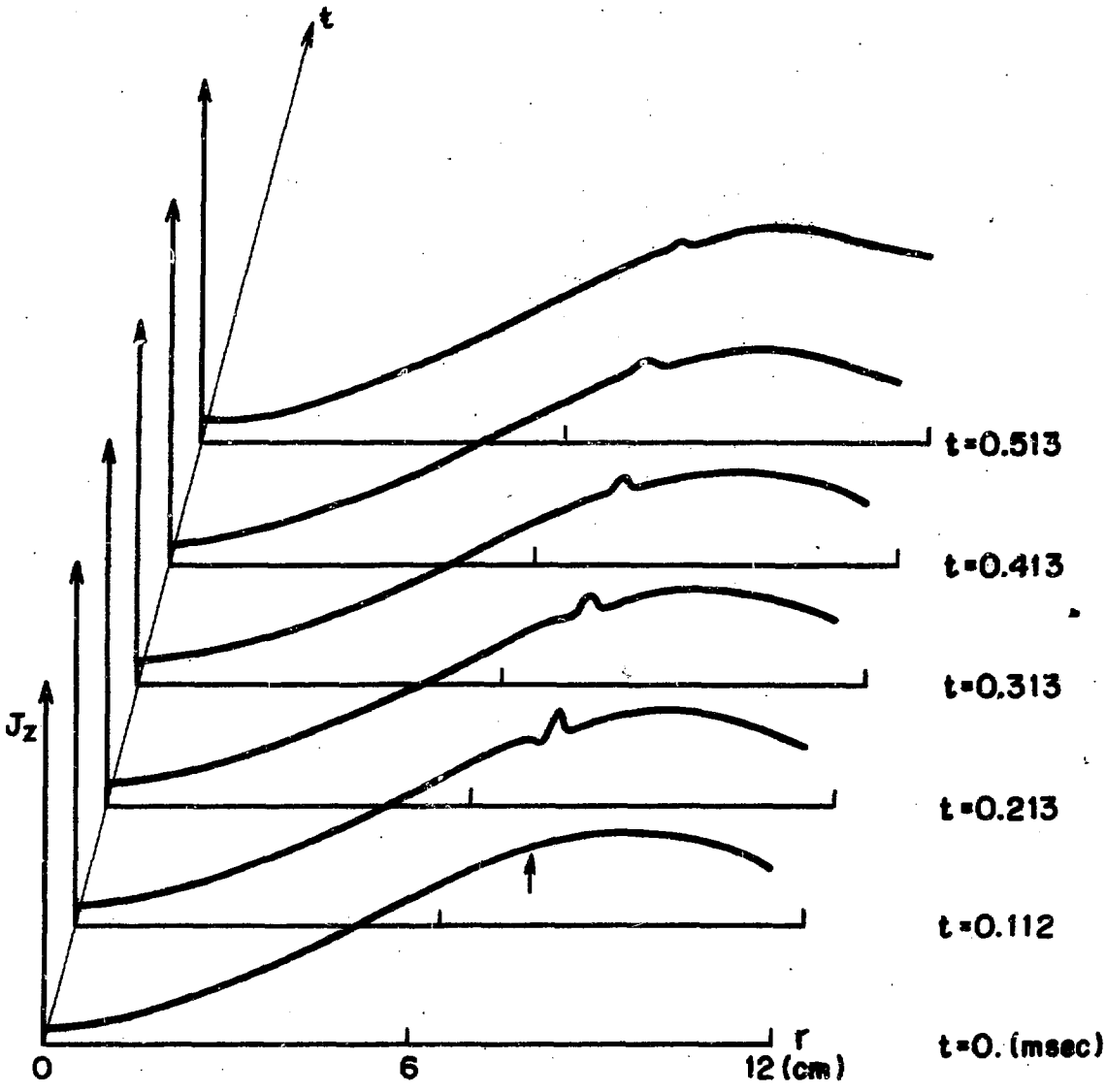


Fig. 2 Variation of toroidal current profile. The initial current profile is skin-like. The arrow at t = 0 indicates the position of q = 2 surface.